

Radio-over-fiber transport for the support of wireless broadband services [Invited]

Nathan J. Gomes,¹ Maria Morant,² Arokiaswami Alphones,³ Béatrice Cabon,⁴ John E. Mitchell,⁵ Christophe Lethien,⁶ Mark Csörnyei,⁷ Andreas Stöhr,⁸ and Stavros Iezekiel^{9,*}

¹Department of Electronics, University of Kent, Canterbury, CT2 7NT, United Kingdom

²Valencia Nanophotonics Technology Center, Universidad Politécnica de Valencia, Camino de Vera, s/n, 46022, Valencia, Spain

³School of Electrical and Electronic Engineering, Nanyang Technological University, Singapore 639798

⁴L'Institut de Microélectronique Electromagnétisme et Photonique et le Laboratoire d'Hyperfréquences et de Caractérisation, MINATEC-INPG 3 Parvis Louis Néel, BP 257, 38016 Grenoble Cédex, France

⁵Department of Electronic and Electrical Engineering, University College London, Gower Street, London, WC1E 6BT, United Kingdom

⁶Institut d'Electronique, de Microélectronique et de Nanotechnologie, UMR 8520, Université des Sciences et Technologies de Lille, Avenue Poincaré, BP 60069, 59652 Villeneuve d'Ascq, France and Research Federation, Institut de Recherche sur les Composants Logiciels et Matériels pour l'Information et la Communication Avancée, FR 3024, Parc Scientifique de La Haute Borne, 50 Avenue Haley, 59652 Villeneuve d'Ascq, France

⁷Department of Broadband Infocommunications and Electromagnetic Theory, Budapest University of Technology and Economics, Goldmann Gy. tér 3, Budapest, 1111, Hungary

⁸Universität Duisburg-Essen, Optoelektronik, Lotharstrasse 55, 47057 Duisburg, Germany

⁹Department of Electrical and Computer Engineering, University of Cyprus, 75 Kallipoleos Avenue, P.O. Box 20537, Nicosia 1678, Cyprus

*Corresponding author: iezekiel@ucy.ac.cy

Received August 29, 2008; revised December 1, 2008;

accepted December 1, 2008; published January 20, 2009 (Doc. ID 100441)

Some of the work carried out within the EU Network of Excellence ISIS on radio-over-fiber systems for the support of current and emerging wireless networks is reviewed. Direct laser modulation and externally modulated links have been investigated, and demonstrations of single-mode fiber and multi-mode fiber systems are presented. The wireless networks studied range from personal area networks (such as ZigBee and ultrawideband) through wireless local area networks to wireless metropolitan area networks (WiMAX) and third-generation mobile communications systems. The performance of the radio-over-fiber transmission is referenced to the specifications of the relevant standard, protocol operation is verified, and complete network demonstrations are implemented. © 2009 Optical Society of America

OCIS codes: 060.0060, 060.5625.

1. Introduction

Radio over fiber (RoF) has become of increasing interest for the transport of wireless signals [1]. Radio over fiber can provide a number of advantages for wireless signal distribution, such as improved coverage through the use of low-power distributed antennas, transparency and flexibility, trunking efficiency gains, and lower cost of deployment [2]. Within the European Network of Excellence ISIS (Infrastructures for broadband access in wireless/photonic and integration of strengths in Europe) [3], partners have investigated radio-over-fiber transport of various wireless signal types, ranging from those proposed for personal area networks (PANs), through wireless local area networks (LANs), and particularly the ubiquitous WiFi networks, to metropolitan and wide area networks (MANs and WANs). Of course, although novel radio-over-fiber techniques may have been used, or experiments may have been testing the boundaries for the use of low-cost components, where transmission of standard wire-

less signals has been demonstrated, performance is always measured using metrics for the wireless signals specified in the standards documents. Usually, such performance is specified in terms of error vector magnitude (EVM) in the multilevel signal constellation points, but the signal-to-noise ratio (SNR) and bit-error rate (BER) are also physical layer performance metrics. However, the standards also specify higher layer protocol operation, and in this paper, studies of such effects in radio-over-fiber systems are also presented. The paper is structured as follows: in Sections 2–4, experiments on the physical layer performance of wireless PANs, LANs, and MANs/WANs, respectively, are presented. In Section 5, the performance limitations of a high-quality radio-over-fiber link using an external modulator are theoretically exposed. In Section 6, the higher-layer protocol effects that have been observed for wireless LAN transport over fiber are discussed, while in Section 7 the demonstration of a wireless sensor network using radio over fiber is presented. Section 8 describes the demonstration of 60 GHz RoF systems transmitting broadband data up to 12.5 Gbits/s for potential applications in home area networks (HANs). Medium-range outdoor transmission at several Gbits/s has also been achieved. Finally, the work is summarized in Section 9.

2. Radio-over-Fiber Link Experiments: PANs

There is currently great interest in ultrawideband (UWB) communications for future PANs. The growing interest in UWB is due to its excellent coexistence with other licensed and unlicensed wireless services, its low radiated power, its tolerance to multipath fading, and its low probability of interception due to its wide spectrum and low energy.

UWB wireless transmission technology targets short-range high-bit-rate communications, potentially exceeding 1 Gbit/s. In this section several experiments using UWB technology are reported. In the first case, the use of the impulse-radio (IR) technique is used in a scenario that could be seen as a viable solution for the distribution of high-definition audio and video content in fiber-to-the-home (FTTH) networks. A high-bandwidth external optical modulator and standard single-mode fiber (SSMF) are used for IR-UWB transmission over up to 60 km of fiber. In the second experiment, a single-mode vertical-cavity surface-emitting laser (VCSEL) is used for IR-UWB transmission in conjunction with frequency upconversion. Although only upconversion up to low frequencies is demonstrated, the principle could be applied to upconversion to millimeter-wave frequencies where the radio spectrum of interest for such applications exists (such as the 62 to 66 GHz band). The third experiment examines the transmission of multiband orthogonal frequency division multiplexed (MB-OFDM) UWB signals for indoor fiber installations that are typically based on multimode fiber (MMF), VCSELs operating at 850 nm, and low-cost receivers.

2.A. IR-UWB over Fiber

Figure 1 shows the experimental setup to evaluate the IR-UWB signal degradation due to fiber transmission. IR-UWB monopulses are generated from a 10 GHz Gaussian pulse train (full width at half-maximum=2.8 ps) generated by a mode-locked laser. The pulse train is gated by a Mach–Zehnder modulator (MZM) with 1.25 Gbits/s pseudorandom binary sequence (PRBS) data. The gated optical pulses are photodetected, monopulse shaped (full width at half-maximum=283 ps) by a pulse-shaping filter, and upconverted with a local oscillator (LO) to 6.6 GHz for fiber transmission. The overall –10 dB bandwidth is 3.2 GHz, as shown in Fig. 2(a), and occupies the band from 5 to 8.2 GHz, following current UWB regulations [4]. UWB signals must meet stringent equivalent isotropic radiated power (EIRP) limits [5], shown by the dashed line of Fig. 2(a). The electrical signal and the pulse profile transmitted are shown in Fig. 2(b).

The average optical power at point (2) in Fig. 1 is adjusted to –2 dBm. The IR-UWB signal modulates a 20 GHz bandwidth MZM biased at quadrature. Measurements were carried out back to back and for three FTTH paths of 25, 50, and 60 km reach, as indicated in Fig. 1. Inline amplification is realized by a 23 dB gain erbium-doped fiber amplifier (EDFA) with 4 dB noise figure (Keopsys BT2C-13). The receiver includes an EDFA (Exelite SFA-19) of 4.5 dB noise figure and 19 dBm saturation power. After

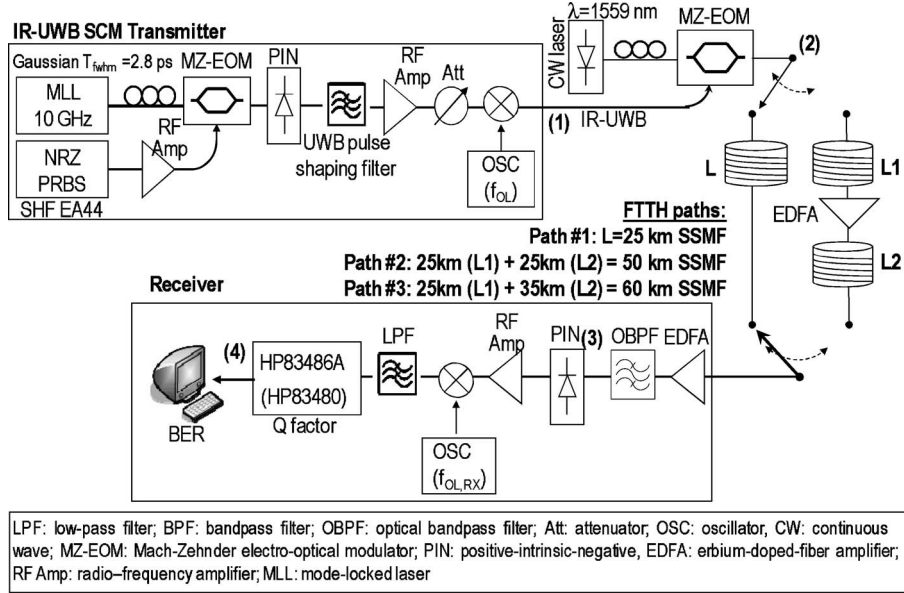


Fig. 1. IR-UWB transmission in FTTH demonstration setup.

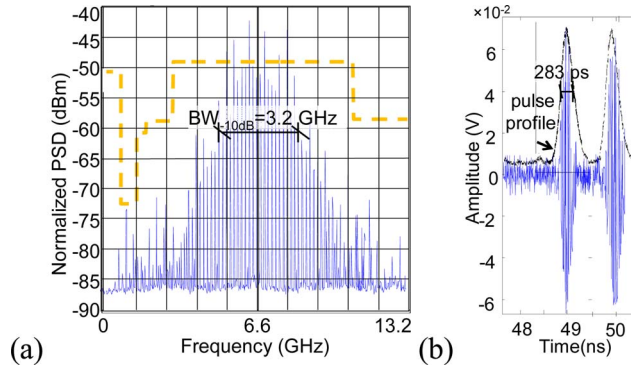


Fig. 2. IR-UWB (a) RF spectrum, (b) electrical signal and pulse profile. PSD, power spectral density.

transmission, the signal is filtered by a 0.8 nm wide (at -0.5 dBo) optical filter and detected by a PIN photodiode (with a responsivity of 0.65 A/W and 50 GHz bandwidth).

Figure 3 shows the BER calculated from the measured Q factor according to BER

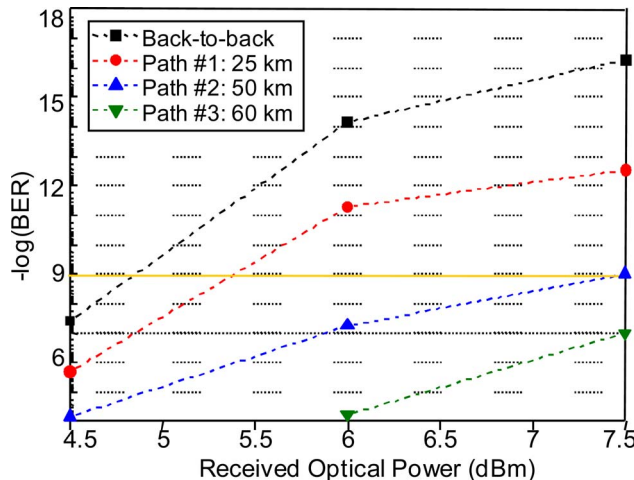


Fig. 3. IR-UWB BER versus optical power for different RoF SSMF paths.

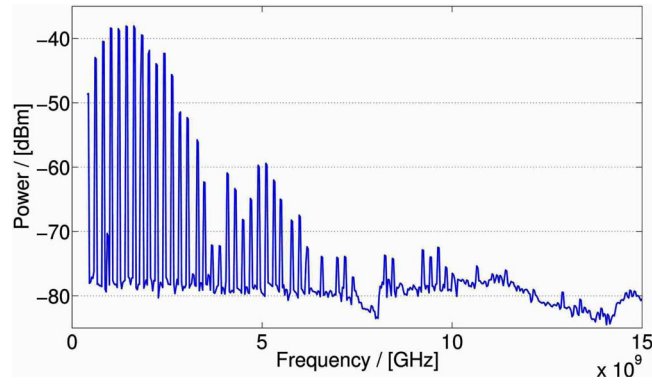


Fig. 4. Measured spectrum of the monocycle at baseband after fiber transmission.

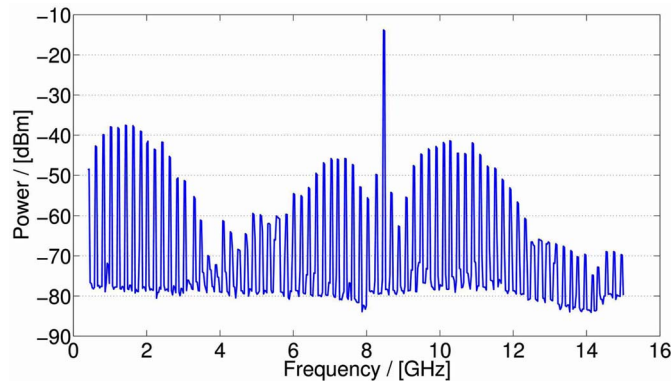


Fig. 5. Measured upconverted spectrum at the output of the fiber link. The monocycle is present at baseband and around the local oscillator at $f_{LO}=8.5$ GHz.

$=0.5 \times \text{erfc}(Q/\sqrt{2})$. Transmission up to 50 km of SSMF is achieved with a BER of 10^{-9} . These experimental results therefore demonstrate the feasibility of radio-over-fiber distribution of 1.25 Gbits/s IR-UWB.

2.B. IR-UWB over SSMF and Upconversion

Here, IR-UWB pulses are upconverted for transmission over 1 m of SSMF with a directly modulated laser diode. A low-cost, single-mode VCSEL at 1550 nm having a relaxation frequency of 8.5 GHz was used to demonstrate the feasibility of upconverting a monocycle while retaining a high resemblance. The results are essentially the same for lengths of SSMF up to 100 m.

The UWB monocycle was generated using a 3.3 Gbits/s pulse pattern generator with a pulse full width at half-maximum (FWHM) of approximately 310 ps and a repetition rate of 4.8 ns and transmitted along the SSMF. The back-to-back photodetected spectrum shown in Fig. 4 exhibits a 3 dB bandwidth of 1.7 GHz between 800 MHz and 2.5 GHz, this being for a VCSEL bias current of $I_{\text{bias}}=2.3$ mA [in the linear part of its light-current (L-I) static characteristics]. To reject spurious power at frequencies above 5 GHz, a low-pass filter with a cutoff frequency of $f_c=5.2$ GHz was used.

Frequency upconversion was then performed using the nonlinearity of the VCSEL and a local oscillator at a frequency of 8.5 GHz while adjusting the bias for optimum frequency conversion. The results of Fig. 5 were obtained at $I_{\text{bias}}=3$ mA and show that the baseband signal has been upconverted with the upper sideband located between 9.3 and 11.0 GHz with a 8.5 GHz LO.

Two bias currents were set: $I_{\text{bias}}=3$ mA, and in the saturation region $I_{\text{bias}}=6$ mA. A comparison is made between the monocycles before transmission and after upconversion to 8.5 GHz; transmission and subsequent downconversion with an electrical mixer back to baseband are shown in Fig. 6 for the case of $I_{\text{bias}}=3$ mA. The $I_{\text{bias}}=3$ mA case was chosen after evaluating the Pearson product-moment correlation coefficient (MCV [6]) between the emitted and received pulse after upconversion, which led to a maximum correlation coefficient of $\rho=0.94$ and 0.76 for $I_{\text{bias}}=3$ mA and 6 mA, respectively.

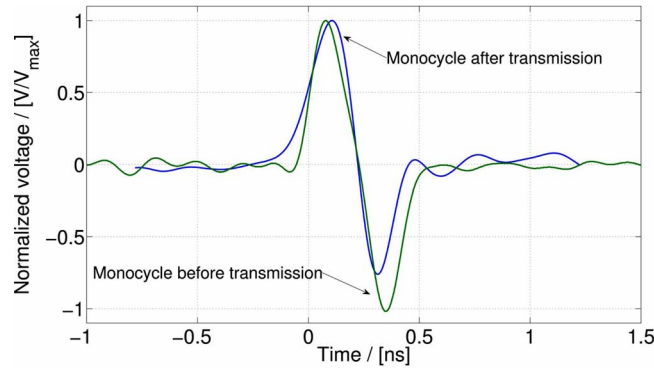


Fig. 6. Original baseband monocycle and after upconversion at 8.5 GHz, $I_{bias}=3$ mA.

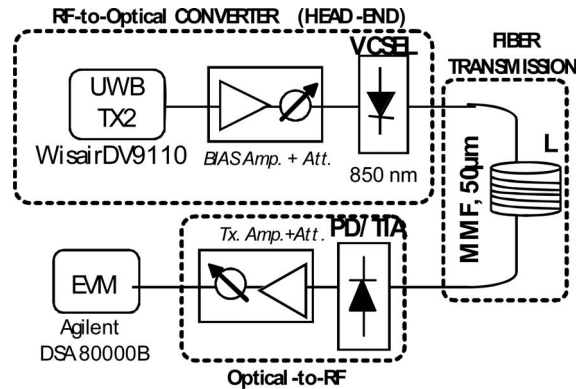


Fig. 7. Experimental setup for performance analysis of MB-OFDM UWB on fiber.

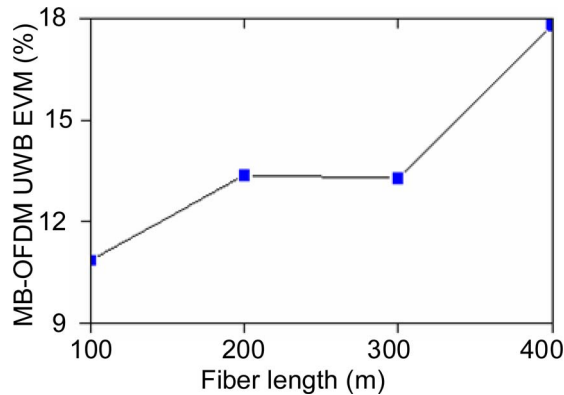


Fig. 8. MB-OFDM UWB EVM results for different MMF lengths.

2.C. MB-UWB over Fiber

Figure 7 shows the experimental setup used to evaluate the performance of the transmission of standard MB-OFDM UWB, as defined in international standard ECMA-368 [4], over multimode fiber.

Figure 8 shows the measured EVM when UWB-OFDM signals are transmitted through 100, 200, 300, and 400 m lengths of multimode fiber (MMF). The quality of the UWB signal degrades quickly due to the modal dispersion at higher frequencies. Nevertheless, EVM results after transmission through 400 m of fiber satisfy the ECMA-368 standard requirements of 18.84% EVM [4].

3. Radio-over-Fiber Link Experiments: Wireless LANs

In this section, the transmission of the now ubiquitous IEEE wireless LAN signals over fiber is investigated. Two contrasting experiments are presented: in the first,

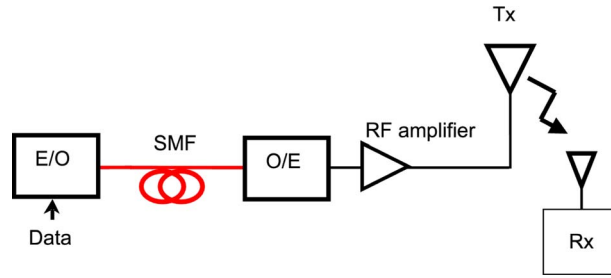


Fig. 9. Typical implementation of a radio-over-fiber system.

upconversion following that presented for IR-UWB in the previous section is applied, again with a view to providing a proof of principle for future millimeter-wave systems; in the second, low-cost VCSEL MMF links (including both glass and polymer fiber types) are investigated, primarily with a view to in-building distribution systems.

3.A. 802.11a and Upconversion

For similar reasons as for the upconversion of the IR-UWB signals, here the transmission and upconversion to 5.1 GHz of a wireless LAN (WLAN) IEEE 802.11a signal over 2 m of SSMF is investigated. The radio-over-fiber link shown in Fig. 9 transports an analog radio signal to a remote antenna, where the detected electrical signal after the RF amplifier can be transmitted without further processing. However, frequency upconversion is necessary in future WiMax systems (for example) since they can exploit the 2 to 66 GHz band. As in Section 2, the nonlinearity of a low-cost 1550 nm single-mode VCSEL diode is exploited to perform upconversion, thus overcoming its intrinsic bandwidth limitation. A LO at $f_{LO}=2$ GHz was used for frequency upconversion; together with the WLAN data, it directly modulates the VCSEL.

The quality of the signal after the upconversion process was evaluated by measurements of the root-mean-square (rms) EVM of the constellation points. The commercial software package Advanced Design System was used to generate the complex waveforms of a WLAN 64-QAM (quadrature amplitude modulated) IEEE 802.11a OFDM signal at a bit rate of 54 Mbits/s, occupying a band of 20 MHz. The waveforms were subsequently uploaded to an Agilent vector signal generator ESG E4438C, which performs modulation of a carrier frequency of $f_{RF}=1.1$ GHz. The EVM was evaluated at the output of the system by vector signal analyzer (VSA) software running on an Agilent digital sampling oscilloscope (DSO).

The desired mixing product is $f_{RF}+2f_{LO}$ and is at 5.1 GHz after the optical-microwave mixing process, where the RF signal is the WLAN signal. As in Section 2, the bias current of the VCSEL was set to $I_{bias}\approx 3$ mA to optimize mixing. The goal was to minimize the EVM while maximizing the upconverted power to the desired intermodulation frequency. To achieve this, optimization of the values of the bias current I_{bias} , the injected RF power P_{RF} of the WLAN signal, and the local oscillator power P_{LO} was required.

Figure 10 shows the strong influence of P_{LO} on the measured EVM. For a high

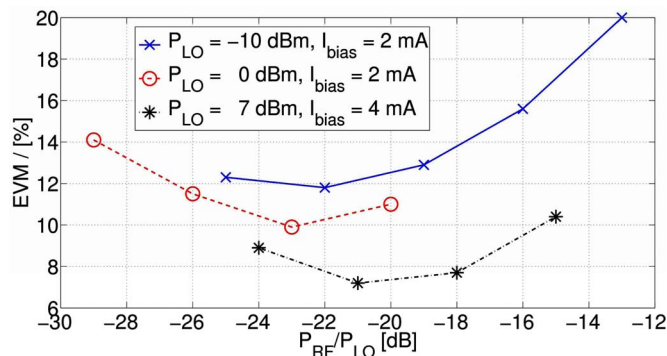


Fig. 10. Measured EVM after upconversion to $f_{RF}+2f_{LO}=5.1$ GHz as a function of the power ratio P_{RF}/P_{LO} between the RF signal and the local oscillator.

Table 1. MMF Specifications^a

Fiber type	Corning Multimode Fibers			
	SX50	SXi50	SXp50	SX62.5
Standard compliance ISO	OM2	OM2	OM3	OM1
Standard compliance IEC	A1a.1	A1a.1	A1a.2	A1b
Standard compliance TIA	492AAAB	492AAAB	492AAAC-A	492AAAA-A
BL product (MHz·km) at 850 nm	510	850	2000	385
Core/cladding diameters	50/125	50/125	50/125	62.5/125

^aAccording to the IEC 60793-2-10/TIA/ISO 11801 standards.

injected LO power ($P_{LO}=7$ dBm), the upconversion becomes less sensitive to the exact value of bias current, saturating at an optimal EVM value of 7.4%, which is a very acceptable value in the standard.

3.B. Multimode Fiber Links for IEEE 802.11g

Here, experimental results on the transmission of the IEEE 802.11g standard over low-cost MMF-based radio-over-fiber links for in-building applications are described. WLAN over MMF technology allows transfer of IEEE 802.11g signals using a picocellular network architecture in order to enhance the indoor coverage (wireless range, highest achievable data rate) while using preinstalled fiber networks. The IEEE 802.11g standard operates at 2.4 GHz and data transmission is based on 64-QAM-OFDM modulation for the transmission of up to 54 Mbits/s over 100 m free space. Nevertheless, this throughput is drastically reduced (less than 10 Mbits/s in several cases) in confined spaces such as in a building due to the propagation channel properties (including wall and floor material reflection and absorption and multipath effects). The use of a multiple picocell concept (with a wireless range of approximately 10 m) enhances the quality of service of the IEEE 802.11g for indoor distribution (making 54 Mbits/s data rates achievable over all of the building). For coverage with picocells, a low-cost approach is necessary, leading to the use of the intensity modulation–direct detection technique (IM-DD) without sophisticated circuitry, multimode fibers either in glass or polymer, and off-the-shelf optoelectronic converters (VCSELs, photodiodes). According to [7], most in-building networks are based on multimode fiber (90%). New multimode fiber based on the $\text{SiO}_2/\text{GeO}_2$ material line, such as that produced by Draka Comteq [8] or Corning [9], has exhibited extended modal bandwidth (bandwidth–length product >2 GHz·km at 850 nm) allowing the transmission of radio signals with higher RF subcarrier frequency (up to 10 GHz) over longer distances (500 m).

Such glass multimode fibers enable a good trade-off between cost and performance; the measured physical parameters of selected fibers are summarized in Table 1. Nevertheless, to decrease the optical connection costs of radio-over-fiber networks and targeting a do-it-yourself installation concept, novel optical fibers based on an amorphous fluoropolymer (CYTOP) material have been developed by Asahi Glass [10] and Chromis Fiberoptics, Inc. [11], with core diameters between 50 and 120 μm and bandwidth–length products greater than 500 MHz·km at 850 nm. They are designed to be used in short-haul and high-bit-rate networks but suffer from high attenuation between 850 and 1300 nm (~ 45 dB/km).

The IM-DD WLAN over multimode fiber transmission scheme is shown in Fig. 11. In terms of optoelectronic components, the uplinks and downlinks are identical and are composed of a laser (typically an 850 nm multimode VCSEL) and a photodiode. Concerning the electronic components, RF amplifiers, which are different for uplink and downlink, are used in conjunction with a WLAN antenna.

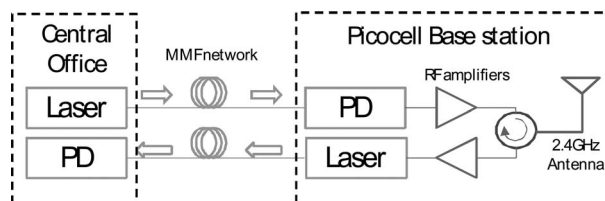


Fig. 11. Radio over multimode fiber using IM-DD for WLANs.

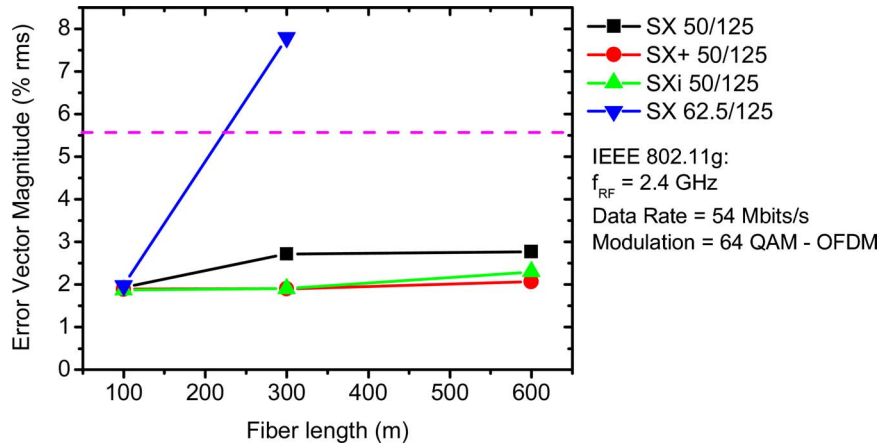


Fig. 12. EVM measured as a function of fiber length [12].

The link performance has been characterized through EVM measurement as a function of fiber length for all the fibers (see Table 1) under consideration; these results are presented in Fig. 12. The EVM (rms) required for IEEE 802.11g transmission must be less than 5.6% for the whole path (i.e., including both optical and wireless paths). Thus, lower EVM in the optical link will allow for a higher EVM budget in the wireless path. For all the 50 μm core diameter fibers, the EVM remains at around 2.5% for link lengths up to 600 m. By contrast, the 62.5 μm core diameter fiber-based transmission exhibits a high EVM value prohibiting its use for almost all link lengths [10]; the EVM exceeds the minimum requirement (5.6%) at around a 200 m link length due to the relatively low bandwidth-length (BL) product at 850 nm (385 MHz·km) of this fiber type. Improved link performance might be achievable using this fiber at 1300 nm wavelength (since it is optimized for this wavelength).

The measurement of EVM as a function of RF input power at the laser input has been carried out for a 300 m link length in order to determine the RF power range giving rise to the lowest EVM value and so to fix the gain of the RF amplifiers that are inserted in the respective links (uplinks and downlinks). As can be seen from the results in Fig. 13, the RF power range is large; it is between -20 and 0 dBm. The EVM is relatively flat over this power range corresponding to the best transmission case. When the RF power level launched into the VCSEL is too high, it induces distortion in the radio-over-fiber system and so the EVM increases quickly. The 64-QAM-OFDM signal is very sensitive to the peak-to-average power ratio (PAPR) and the input 1 dB compression point of the radio over multimode fiber link (measured as 3 dBm) is not sufficient to allow the transmission of such high-power signals (>-2 dBm) without degradation.

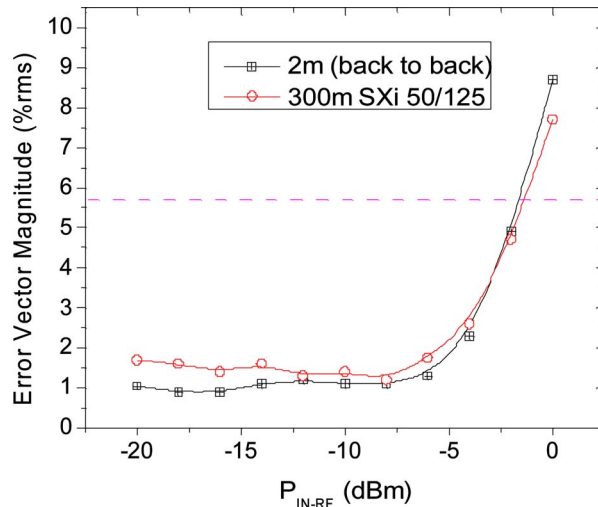


Fig. 13. EVM as a function of the RF power level for the 2.4 GHz radio-over-fiber link.

3.C. General Discussion on Multiple System Configurations and Remote Powering

Radio-over-fiber distribution of WLAN signals allows flexible system architectures in which the signals from co-located WiFi access points can be transported to and from multiple remote access units (RAUs) to improve coverage or can be combined and transported to individual RAUs to improve capacity in traffic hot-spot areas [13]. In addition, the signals of other standard systems such as PANs (as discussed in Section 2) and WiMAX and mobile communications systems (as discussed in Section 4) can be transported to the same RAUs, permitting cost sharing between the systems. When multiple systems are to operate over the same radio-over-fiber links, two general options are possible in the design of the RAUs [13]. In the first, the signals use common amplifier chains in the RAU: this may minimize cost but does not allow for optimization of the power and noise budget according to each system’s requirements, and the requirements for a Global System for Mobile Communication (GSM) type system using Gaussian minimum shift keying modulation, which is very tolerant to system nonlinearities, are very different from those of an OFDM-type system such as IEEE 802.11a/g, which is very susceptible to nonlinear effects (as shown in the previous subsection). Cost reduction might also be lessened by the fact that wider bandwidth amplifiers (covering all required systems) and higher performance (e.g., in terms of third-order intercept points) might be required. The alternative is to separate the amplifier chains for the different systems as far as possible. The intermodulation products can also be removed by RF filtering in such a scheme. The problem then becomes the increased component count, and, most likely, increased cost. Power consumption will generally also increase with the increased component count. Interesting work has been carried out on powering low-cost RAUs optically, using power-over-fiber links [14]. This is eminently suitable for the simpler, low-component-count RAU approach. Finally, as has been discussed in [13], it may not be necessary to optimize for equal wireless distances for all systems. Whereas WLAN signals may be sent to and from all (or nearly all) RAUs, mobile communication system signals may be sent to and from fewer RAUs taking advantage of the generally greater wireless distances possible with similar transmit and receive power levels and of the lesser demand on these systems for high-bandwidth services.

4. Radio-over-Fiber Link Experiments: Wireless MANs and 3G

A key enabler for supporting very high data rates and many users in advanced networks is the reduction in cell size. This is apparent for 802.16 WiMAX and third-generation (3G) mobile communications, with picocellular system design being proposed. Radio-over-fiber distribution has been proposed for such systems, and for in-building distribution, multimode fiber is considered attractive for moderate distance transmission up to some hundreds of meters. In this section, we examine radio-

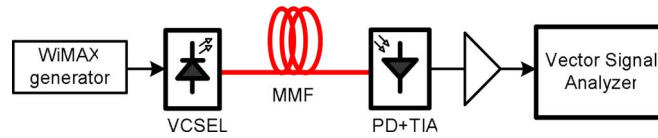


Fig. 14. Measurement setup for WiMAX over MMF.

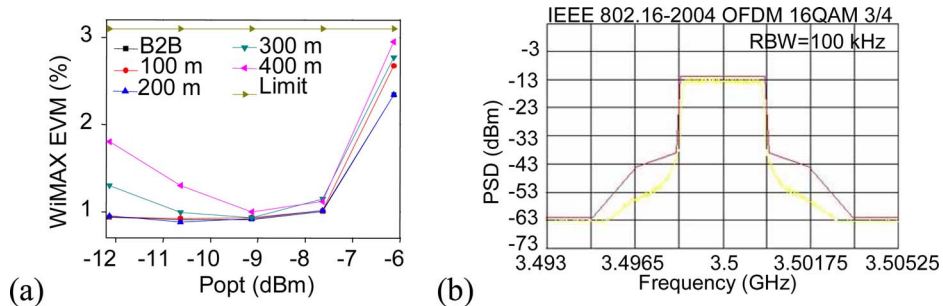


Fig. 15. (a) WiMAX EVM measurements results and (b) measured conformance with spectral mask.

over-multimode-fiber experiments for WiMAX and 3G systems that use low-cost, short-wavelength (850 nm) VCSELs and multimode fiber.

4.A. WiMAX over Fiber

The experimental setup for the WiMAX work is shown in Fig. 14. Measurements using a 3.5 MHz 64-QAM 3/4 WiMAX signal at the 3.5 GHz operating band over different fiber lengths up to 400 m are shown in Fig. 15. The signal quality (EVM) measurements at the antenna in Fig. 15(a) show that the EVM remains below the limit of 3.1% imposed by the standard for the corresponding 64-QAM modulation. Figure 15(b) shows that the received signal in the experiment complies with the standard spectral mask, necessary to avoid interference in adjacent channels.

4.B. Third Generation Partnership Project (3GPP) and Adjacent Channel Leakage Ratio Testing

Testing of the EVM performance of 3G systems transported over multimode fiber links has also been carried out. In fact, in the experimental setup shown in Fig. 16 [13], multiple systems were transported, although here we concentrate on the results obtained for the 3G system Universal Mobile Telecommunications System (UMTS). The EVM results measured at the antenna port of the downlink are presented in Fig. 17; similar results would be measured in the uplink. As the EVM requirement is

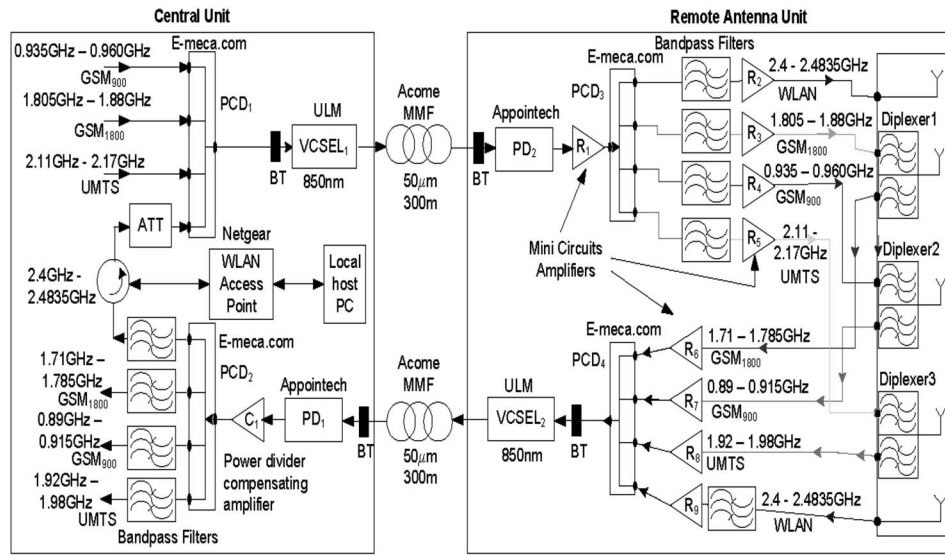


Fig. 16. Experimental setup for multisystem transport over a VCSEL multimode fiber link [13].

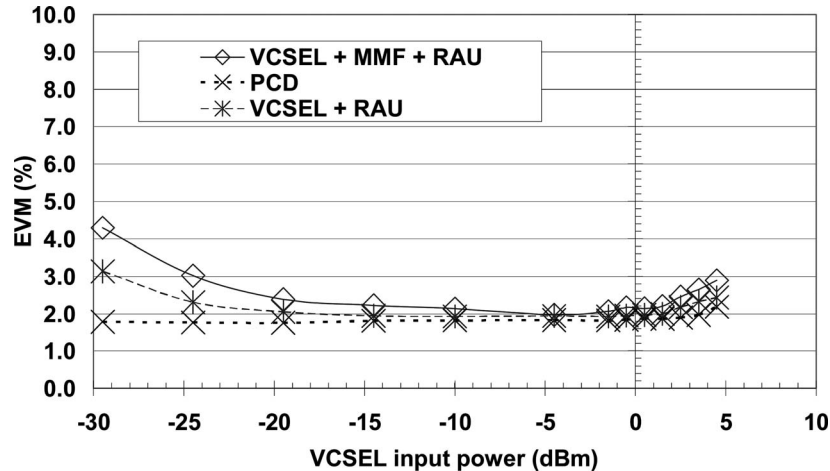


Fig. 17. EVM measurements for downlink UMTS radio-over-fiber transmission in the system of Fig. 16 as a function of central unit VCSEL RF drive power. Note: all other systems are present [13].

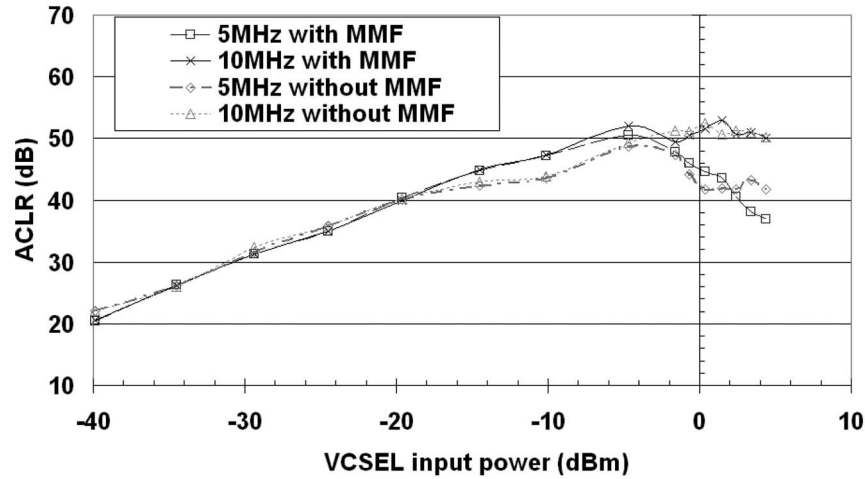


Fig. 18. ACLR measurement for UMTS for the setup of Fig. 16 with all other systems present. The rising part of the curves is within conformance (although they are below the 50 and 45 dB requirements) as noise rather than signal leakage is measured in this region [13].

12.5%, the measurements demonstrate conformance over the whole range and suggest an operational dynamic range of much greater than 35 dB. However, the measurements of the adjacent channel leakage ratio (ACLR) shown in Fig. 18 demonstrate a further limitation often neglected in system experiments. The UMTS ACLR requirements are 50 dB at 10 MHz offset and 45 dB at 5 MHz offset. In the measurements of Fig. 18, the system noise floor is measured until the onset of significant VCSEL non-linearity, which results in the channel leakage. The emitted noise requirement is being met, but in the region at higher power levels where the curves start decreasing, the ACLR is dominant. In the system measured, therefore, the drive power to the VCSEL is limited to less than 0 dBm because of the ACLR requirement (whereas the EVM measurement suggested it could exceed 5 dBm).

5. Externally Modulated Link Modeling for OFDM Signals over Fiber

RoF systems employ a centralized architecture wherein, by delivering the radio signals directly, the optical fiber link avoids the necessity to generate high-frequency radio carriers at the antenna site. Since antenna sites are usually remote from easy access, there is much to gain from such an arrangement [15]. A key aspect of RoF system design is the assessment of modulation formats and OFDM in particular. Early simulation studies focused on examining the feasibility of OFDM in multimode RoF systems for directly modulated [16] and externally modulated links [17].

In this work, the behavior of an OFDM signal in a radio over fiber for WLAN environment has been studied. Figure 19 depicts the RoF system being simulated. A MZM was employed to modulate an optical signal. The MZM transfer function can be represented as given in Eq. (1):

$$\psi[v_1(t)v_2(t)] = 1/2 \exp[j\pi v_1(t)/V_\pi] + \delta/2 \exp[j\pi v_2(t)/V_\pi], \quad (1)$$

where $v_1(t)$ and $v_2(t)$ represent the time-varying electrical signals applied to each electrode of the MZM. V_π is the switching voltage of the MZM and is a constant for a particular device. δ is related to the extinction ratio r measured at the output of the MZM as $(\sqrt{r}-1)/(\sqrt{r}+1)$ [18].

The simulation model is designed with the considerations of a RoF system used to distribute 802.11a WLAN signals [19]. The signal behavior after the remote access point (RAP) has been rigorously modeled, including the channel noise. The performance evaluation simulations were performed on the downlink (i.e., base station to portable device) channel with the assumption that the uplink path is essentially a mirror image of the downlink. The OFDM modulator and demodulator [20] were simulated in MATLAB in accordance with the 802.11a physical layer specifications.

The effect of attenuation and dispersion in the fiber is applied on the signal in the Fourier domain using the transfer function of the fiber [15]:

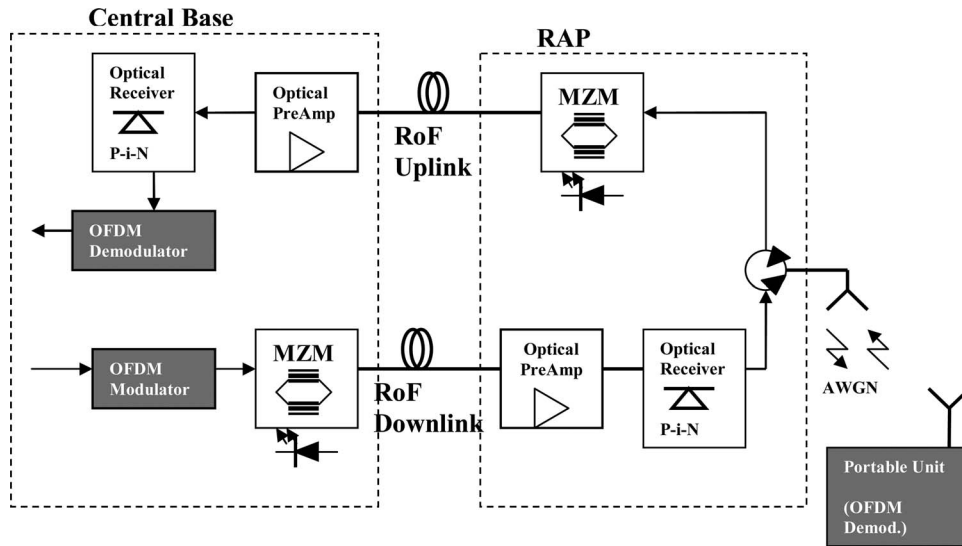


Fig. 19. Externally modulated (MZM) radio-over-fiber system model. AWGN, additive white Gaussian noise.

$$H_r(f) = \exp\{[j\pi DL(\lambda f)^2/c] - (\alpha L/2)\} . \tag{2}$$

Here D is the dispersion parameter, L is the fiber length, λ is the wavelength (i.e., 1550 nm), and α is the attenuation coefficient. Note that we have used a configuration where the amplifier stage follows the fiber rather than vice versa. Even though this results in worse noise figures, with the adoption of this technique we can better model a real dispersive system with suppressed nonlinear effects.

For the fiber transmission of OFDM signals, the signal output can be defined as in [18]:

$$v_{Rx}(t) \propto \{\sin[2\pi v_{sig}(t)]/V_\pi + N_{Rx}(t)R_{out}\} , \tag{3}$$

where R_{out} is the load resistor and $N_{Rx}(t)$ is an average current term that represents the sum of all noise sources present in the received optical signal and was selected to give a relatively high SNR of 20 dB. With the input SNR being held constant, the average carrier amplitude $A_{sig,Av}$ of an OFDM input signal $v_{sig}(t)$ was swept through a range of levels. The same input signal was used at each input level. V_π was set to a

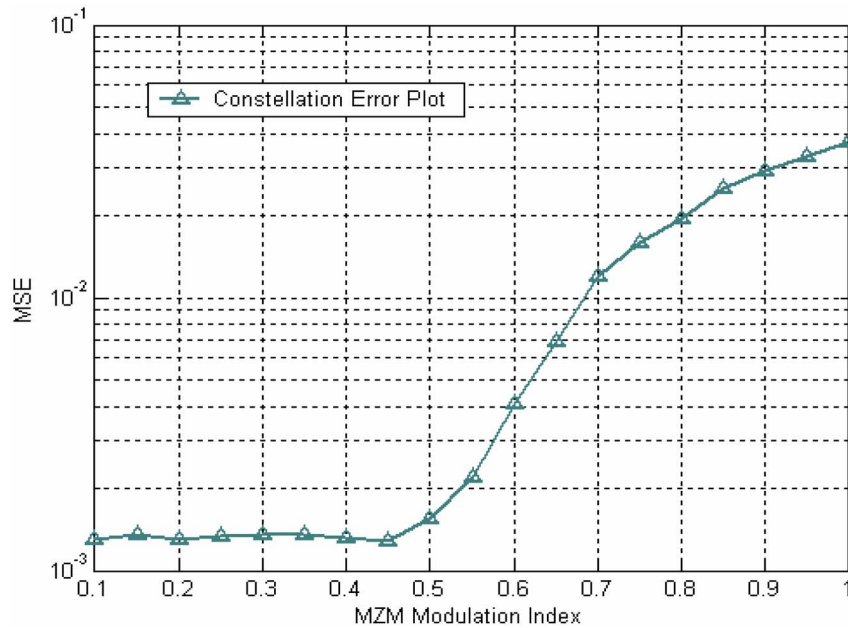


Fig. 20. Constellation error at a nominal MZM bias point.

typical value of 4 V. The MZM is biased at $V_{\text{Bias,Nom}} = V_{\pi}/2$ as in virtually every application in which the device is used. This is the point on the MZM transfer function that is most linear and provides the greatest input/output power efficiency. In Fig. 20, the mean-squared constellation error $\text{MSE}_{\text{Const}}$ is plotted as a function of the modulation index Γ_{MZM} :

$$\Gamma_{\text{MZM}} = A_{\text{sig,Avg}}/0.5V_{\pi} \tag{4}$$

The curve remains essentially constant at a level slightly greater than 10^{-3} for low values of Γ_{MZM} . Constellation degradation increases near $\Gamma_{\text{MZM}}=0.45$ when the $\text{MSE}_{\text{Const}}$ increases rapidly. At this point the signal degradation caused by noise is at a minimum, so this is the optimal operating point for the link.

Figure 21 shows the average optical intensity at the output of the MZM for a given Γ_{MZM} . The result also shows the input signal amplitude as a function of the modulation index. From the observations we see that the received SNR would be significantly increased with an increase in the modulation index above the optimal operating point. In Fig. 22 the simulation results depict the dependence of the BER on the fiber length. Simulation results are extracted without the use of any error correction as well as by using forward error correction (FEC) with a constraint length of 7 as recommended by 802.11a.

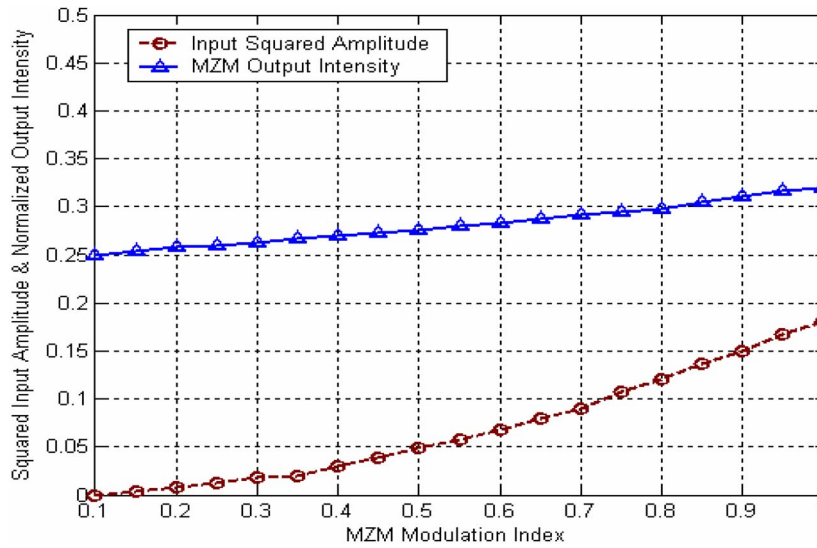


Fig. 21. Signal amplitude and output intensity (nominal bias point).

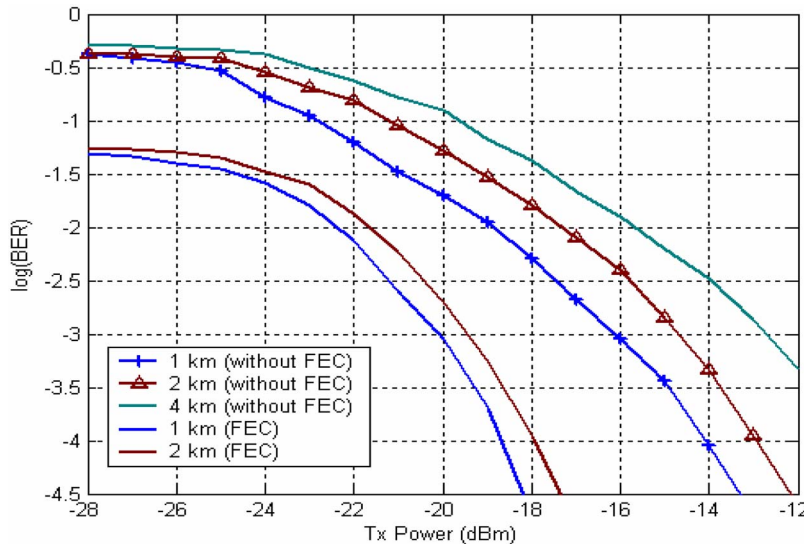


Fig. 22. BER dependence on fiber length.

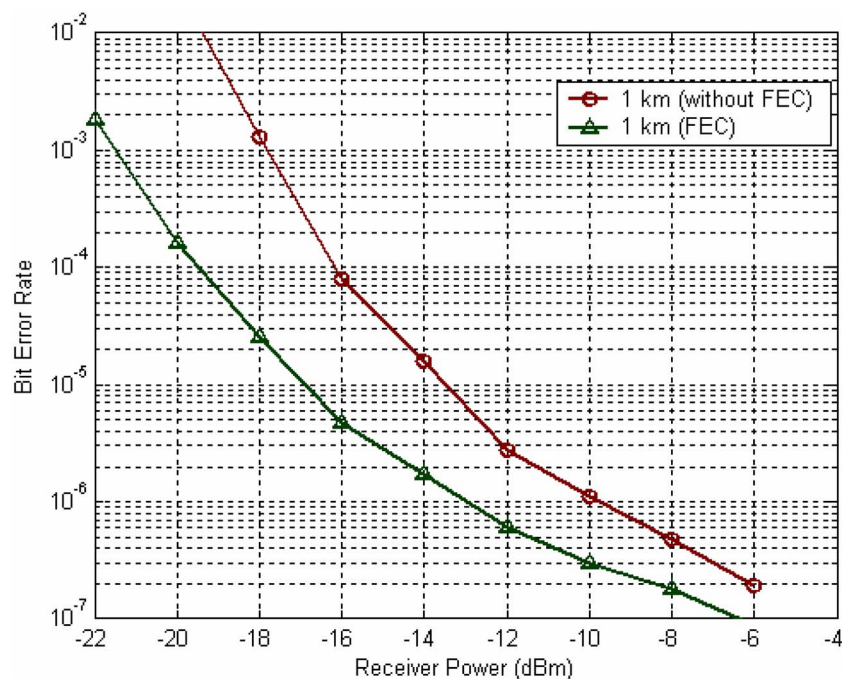


Fig. 23. Receiver performance with FEC.

For the simulated RoF system model, we can see that an input power of -14 to -16 dBm would be ideal to achieve a BER of 10^{-3} to 10^{-4} for a fiber length of less than 1 km, without the use of FEC. We can also expect little performance degradation (with respect to transmitted power) for the longer fiber lengths of 2 and 4 km. While using FEC, a performance gain of approximately 4 dBm is achieved for fiber lengths of 1 and 2 km.

The receiver simulation results shown in Fig. 23 (compared with Fig. 22) show a power loss of 3 to 4 dBm for transmission over a 1 km length of SSMF. From the simulations, it is evident that the receiver sensitivity can be further improved with the use of the FEC techniques of IEEE 802.11a. A receiver power level of -21 to -19 dBm is required for achieving the target BER performance from the system with the use of FEC.

6. Higher-Layer Protocol Issues

Although many experiments at the physical layer (such as those described in Sections 2–4) have demonstrated significant fiber transmission distances, other effects, such as those on the media access control (MAC) protocol, can degrade performance. The protocols defined in a radio standard, for example, the IEEE 802.11 standard implemented in WiFi, at layer 2 or above, such as the Internet protocol (IP), the transmission control protocol (TCP), or the user datagram protocol (UDP), will all interact to determine the total transmission capacity of any radio-over-fiber system.

6.A. Impact of the 802.11 MAC

Considering first the impact of the IEEE 802.11 MAC, it is straightforward to show that the fiber length that can be introduced into the system is limited by the acknowledge (ACK) and clear-to-send (CTS) time-out values implemented by the access point. These time outs, set with the assumption of only a relatively short wireless channel, will expire and result in lost packets if exceeded by the time delay introduced by the addition of optical fiber.

Experimental and simulation-based investigations have been performed to show the expected ranges given minimum and typical time-out values [21,22]. Figure 24 shows results when the distributed coordination function (DCF) basic access mode is used in the downlink, with the case for the uplink being almost identical when only a

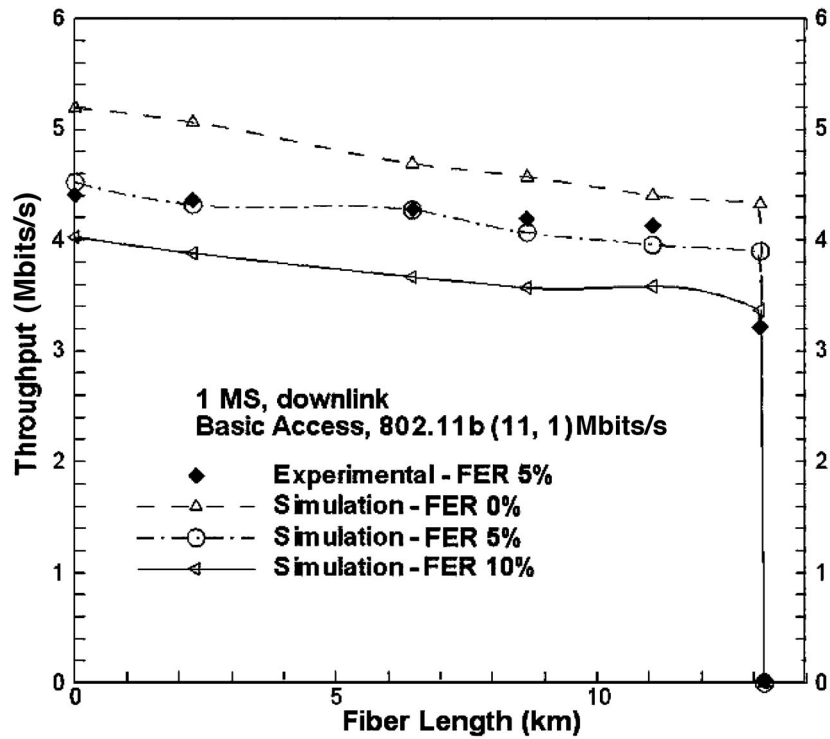


Fig. 24. Variation of throughput with fiber length using basic access.

single station is considered. The experimental setup follows that shown in [23]. Figure 25 shows the same results when the DCF request-to-send/clear-to-send (RTS/CTS) access mechanism is used.

First, it is noted that the throughput is always lower than the data rate (in the example of 802.11b this is 11 Mbits/s) due to the control overhead. The impact of this is exacerbated by all control frames being transmitted at 1 Mbit/s. With the RTS/CTS

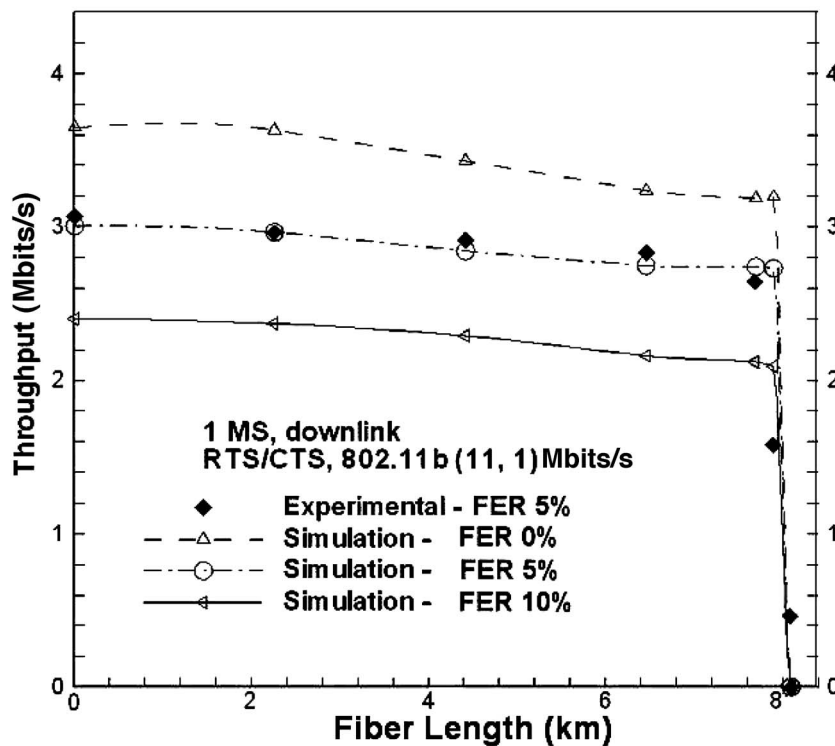


Fig. 25. Variation of throughput with fiber length using RTS/CTS.

access mechanism there is a higher overhead than with the basic access mechanism due to the extra transmission required. As the fiber length is increased, the throughput of the system steadily decreases due to the increased waiting time between packet transfers caused by the fiber propagation. However, there comes a point when the throughput rapidly decreases when the time-out value is exceeded and all packets are assumed to be lost. Channel errors, which cause lost frames as specified by the frame error rates (FERs) shown in Figs. 24 and 25, also affect the performance of the MAC protocol since they increase the number of retransmissions at the MAC level. Experimental measurements show that, due to this, 5%–7% of packets are transmitted at 5.5 Mbits/s.

It has been shown that an increase in the number of contending stations will result in the system’s throughput not reaching the maximum theoretical throughput due to the increase in the number of collisions from simultaneous transmissions [24]. It is known that in a highly contended environment RTS/CTS provides better performance and so is considered here (other schemes can be found in [22]). Figure 26 shows the relative performance of both the basic and RTS/CTS mechanisms for two station and bidirectional transmission. The transmission rate of control frames for the results shown is 1 Mbit/s. We see that the rate of decline is slightly higher for the basic access method, and that, due to a difference in the time-out values for control and data packets, its transmission distance is greater. It is shown that the available capacity is shared between the two stations in an equitable manner.

The new burst-mode transmission mechanisms in the IEEE 802.11e standard require fewer (or even no) acknowledgments. This streamlining of the acknowledgment procedure has been shown to dramatically improve performance when used in radio-over-fiber systems [25], although care must be taken to guard against unduly high frame loss due to noise and errors and collisions when the numbers of acknowledgments are reduced.

6.B. Impact of TCP and UDP

Since the 802.11 MAC provides for retransmissions, retransmissions at the TCP layer may not be necessary. Thus, we consider UDP as an alternative transport protocol to TCP. Figure 27 shows simulation results for throughput comparing TCP and UDP with the maximum achievable throughput when basic access is used in the downlink.

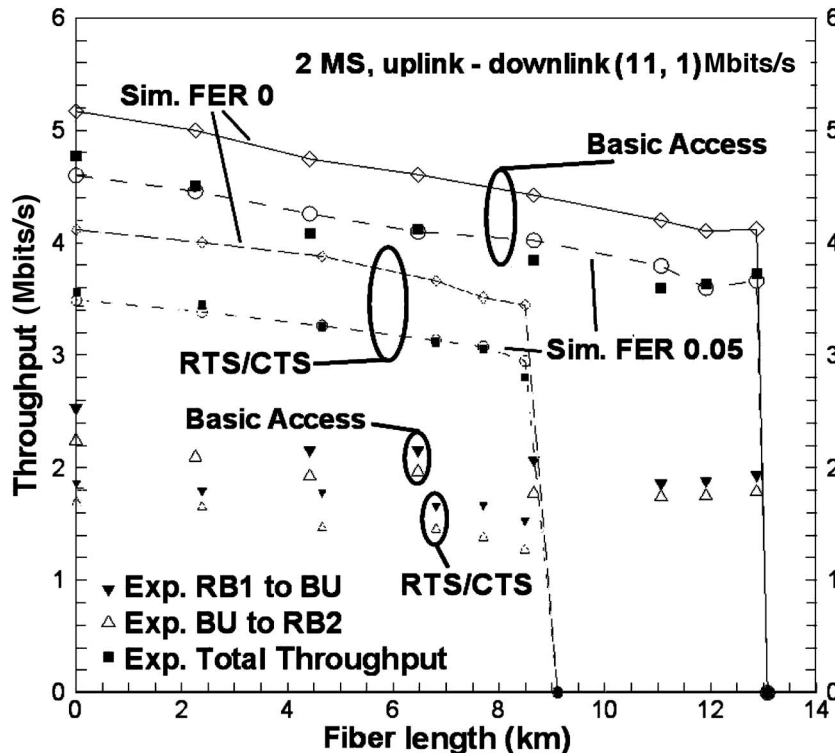


Fig. 26. Variation of throughput with fiber length for TCP transmission (control data rate 1 Mbit/s)

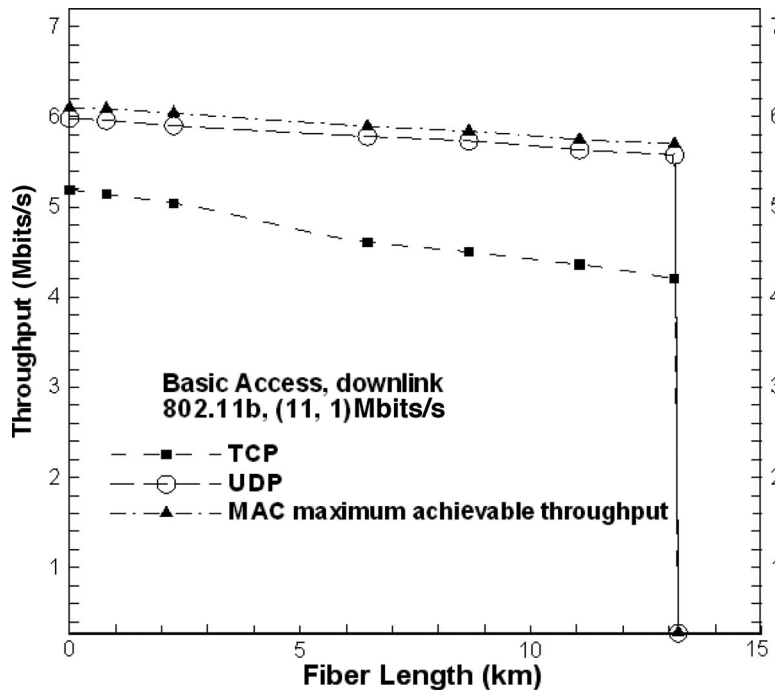


Fig. 27. UDP, TCP, and the MAC maximum achievable throughput simulation results.

It can be seen that the UDP throughput is comparable with that of the MAC itself, whereas the TCP throughput is lower due to the TCP ACK procedure overhead. The slightly higher slope for the TCP case shows that the fiber length adversely affects TCP transmission due to the extra time needed for the TCP ACK procedure. When using the basic access method in a TCP downlink the reduction in throughput increases from 10% when no fiber is used to 15% for 13.1 km of fiber.

7. Demonstration of the Operation of a Complete Sensor Network

Wireless indoor communication systems applying an optical backbone provide an economic and flexible approach for sensor area networks in buildings. In this approach the IEEE-802.15.4-based low-rate wireless communication can be extended by optical cables. The performance of the 802.15.4 ZigBee system is enhanced by the advantages of the combined optical-wireless network solution, such as robustness against electromagnetic interference and flexible subnetwork connections. This method allows for a simple and low-cost indoor communication system [26].

Wireless sensor networks are used in different situations. An important area of concern is home and building monitoring, particularly for fire control and other security aspects. These networks are far more flexible both in installation and in the running operation mode than conventional wired networks. Due to the low data rate (20–200 kbits/s) transmission, defined by the physical and media access layer of the IEEE 802.15.4 standard model, extremely low power consumption (and hence low-cost operation) is feasible. In addition, the low power consumption is supported by the network layer of the transmission, which is defined by the ZigBee Alliance. Due to the network layer operation, the temporarily unused nodes can go over in different doze and sleeping modes, and so the wireless nodes can operate essentially in wireless mode using batteries. This kind of network structure makes the reorganization of the network easy and allows dynamic variation of network structure and function matched to the changing application requirements.

A further advantage of such wireless sensor networks is their self-healing characteristic, which warrants a very simple installation and a highly flexible operation.

In the case of large buildings such as airports and conference centers the cooperation of locally separated networks has special importance. The apparent solution is to use low-cost short-range optical connections, which gives secure information transmis-

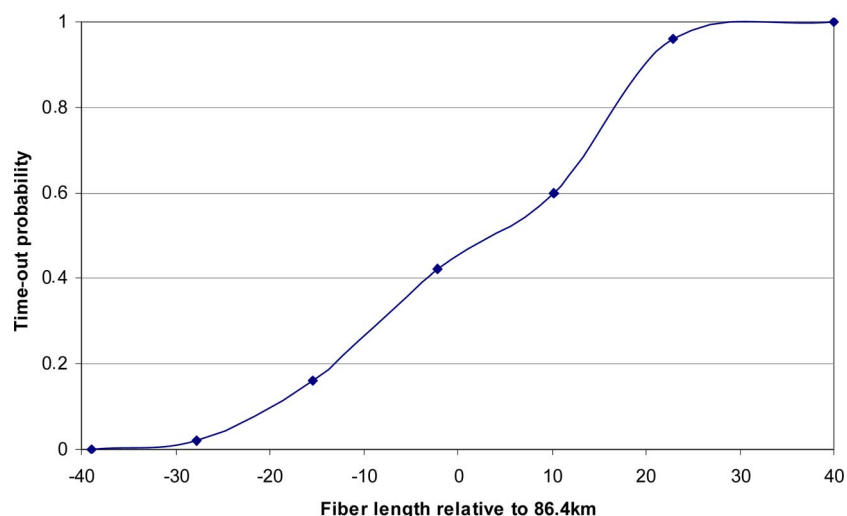


Fig. 28. Time-out uncertainty due to clock jitter.

sion possibility regarding the electromagnetic interference. According to this network scheme, some of the wireless routers of the separated subnetworks are connected via fibers.

In addition, ZigBee has limitations that are rooted in the fundamental principles that created it. One such limitation is the maximum depth of a ZigBee network, as in the maximum number of devices that can join to each other forming a chain, with the ZigBee Coordinator (ZC) at the top. In a ZigBee network, that number is 15; thus the maximum possible diameter of a network is 30, with the ZigBee Coordinator in the center. This limitation is particularly related to the maximum possible operational area of the network. If greater area coverage is necessary, optical links between ZigBee routers present an obvious solution.

The maximum fiber length that can be inserted into the sensor network is limited by the time-out parameters of the MAC layer acknowledgement signals [27]. According to the IEEE 802.15.4 standard, the length of the ACK time out is 54 symbols, which gives a maximum fiber length of 86.4 km (considering 250 kbits/s data speed and 4 bit symbols). The exact value of the maximum fiber length depends on the clock oscillator jitter of the ZigBee sensor devices. In our case we have used an MC13213 system-in-package ZigBee transceiver including an 8 bit microcontroller and the 2.4 GHz ZigBee modem. Considering the 16 MHz clock rate, we could measure an 80 m uncertainty region around 86.4 km in the fiber length between the situation when all ACK packets were received and on the other hand when the communication always collapsed with time-out error. The probability of the MAC layer time-out event is depicted in Fig. 28 as a function of the fiber length uncertainty around 86.4 km.

As shown in Fig. 28, the longest possible fiber link in our ZigBee network is $86.4 \text{ km} \pm 40 \text{ m}$. This kind of time-out uncertainty should be taken into account during optical link deployment in future urban sensor networks, where fiber length of the order of 86 km can easily occur. To avoid failures in operation caused by the time-out uncertainty in a large-scale metropolitan environment, multiple MAC level check measurements are required during deployment to ensure reliable network functioning by keeping off the uncertainty region.

8. Broadband 60 GHz Radio-over-Fiber System Experiments

In this section, we study the potential of radio-over-fiber systems for wireless delivery of very broadband data up to 12.5 Gbits/s by utilizing the large spectrum available for wireless communications in the 60 GHz band [28,29]. Experiments were carried out for indoor home area networks as well as for outdoor access links.

Figure 29 shows the system configuration of the 60 GHz radio-over-fiber link. Basic system parts are the 60 GHz optical carrier generation followed by broadband data modulation, a wireless radio-over-fiber transmitter, and a wireless receiver.

For 60 GHz carrier generation, an external-cavity $1.55 \mu\text{m}$ laser is externally

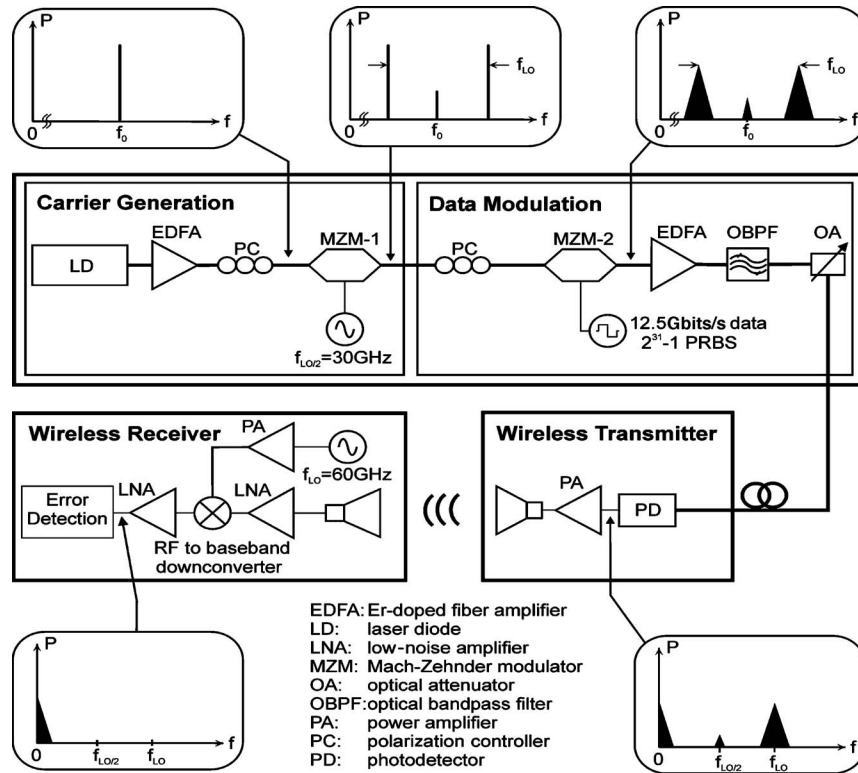


Fig. 29. Schematic of the 60 GHz radio-over-fiber setup.

modulated using a Mach-Zehnder modulator (MZM-1) at a frequency of $f_{LO/2} = 30$ GHz. Bias is set to V_{π} for generating an optical double-sideband-suppressed-carrier (DSB-SC) signal. The optical millimeter-wave signal is subsequently modulated by non-return-to-zero on-off-keying data (NRZ-OOK, $2^{31}-1$) in a second modulator (MZM-2). After fiber-optic transmission to the wireless transmitter via SSMF, the signal is detected by a 70 GHz photodetector. Before wireless transmission with a 20 dBi gain horn antenna, an amplifier is implemented to boost the RF power level up to approximately +11 dBm so as to extend the wireless path length. The signal is received by an identical 20 dBi horn antenna and amplified by a low-noise amplifier (LNA). BER analysis is performed after direct downconversion of the 60 GHz signal to baseband.

For studying the applicability of the constructed system for HANs, short-range indoor tests were carried out, in which the wireless signal was transmitted within a laboratory environment allowing a maximum wireless path length of approximately 11 m. From BER measurements (Fig. 30) we can demonstrate error-free broadband

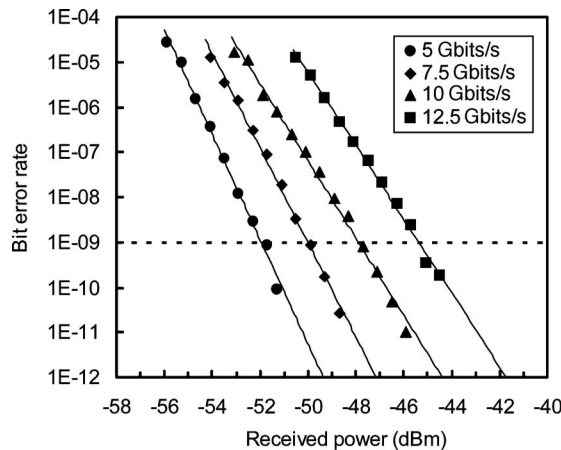


Fig. 30. BERs and 10 Gbits/s eye diagram after 2.5 m wireless transmission.

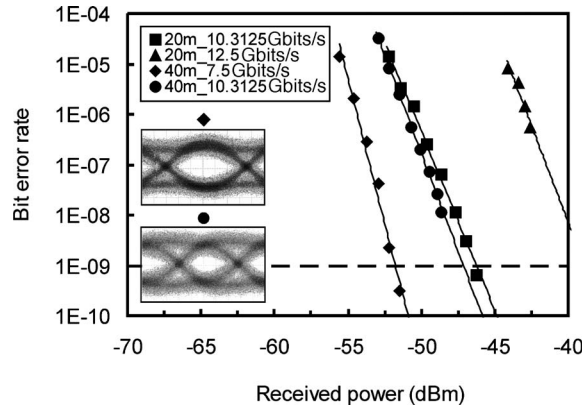


Fig. 31. Measured BER levels for multigigabit data transmission after 20 and 40 m wireless path length.

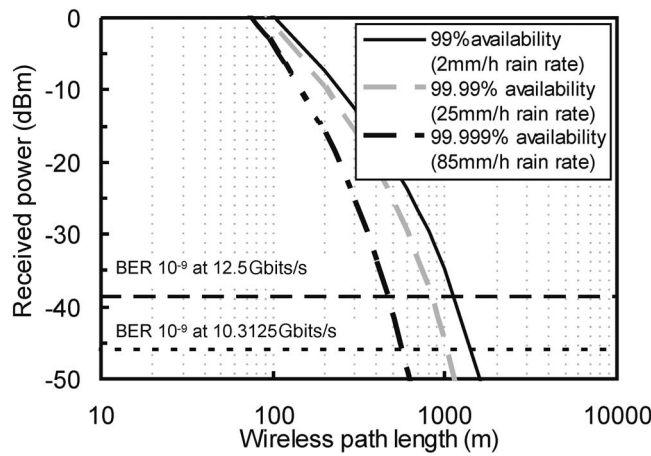


Fig. 32. Maximum wireless path lengths for different weather conditions.

wireless transmission up to 12.5 Gbits/s. No error floor was observed in the BER measurements down to BERs of $<10^{-11}$. For a BER of 10^{-9} ($2^{31}-1$, NRZ) and 2.5 m wireless indoor transmission the measured receiver sensitivity for 10 Gbits/s is -47.6 dBm. We also investigated the maximum wireless path length the system could accommodate at a given data rate to demonstrate the capacity of the constructed system link for short-range indoor communication. Here, we achieved 10 Gbits/s broadband wireless transmission over distances up to approximately 10 m.

For studying access link scenarios, medium-range outdoor experiments were carried out at a height of approximately 120 cm and surrounded by buildings, limiting the maximum wireless path length to 40 m.

Various experiments were carried out for data rates of 7.5 Gbits/s, 10.3125 Gbits/s [gross rate for 64/66 coded 10 gigabit Ethernet (10 GbE)], and 12.5 Gbits/s (gross rate for 8/10 coded 10 GbE). Figure 31 shows BER characteristics after 20 and 40 m wireless transmission and eye diagrams after 40 m wireless transmission. From the results, a sensitivity of -46 dBm for error-free ($\text{BER} < 10^{-9}$) 10.3125 Gbits/s transmission is observed. The system even achieved 12.5 Gbits/s wireless transmission over 20 m. The sensitivity for 10.3125 Gbits/s operation after a 40 m wireless path length is slightly better than for 20 m, which is attributed to reflections from buildings. We expect a general improvement in receiver sensitivity due to reduced multipath propagation, provided the transmitter and receiver are located at a better position, for example, on the roof between two buildings.

Based upon the outdoor experiments, we further studied the potential of extending the wireless path length to the kilometer range by using high-gain antennas such as 50 dBi Cassegrain antennas. Although higher millimeter-wave frequencies in the E- and F-bands offer lower gaseous attenuation, the 60 GHz system under investigation is expected to allow wireless distances up to the kilometer range—even considering

heavy rainfall—provided high-gain antennas are used. Figure 32 shows the received power versus wireless path length by assuming an identical system with the exception of using 50 dBi gain antennas. For the calculations, 60 GHz free-space propagation loss and maximum gaseous attenuation within the 60 GHz band (15.5 dB/km) are assumed. To implement the link availability with respect to rain attenuation under different weather conditions, sample rain data from a central European country were chosen. The corresponding sensitivities for achieving a BER of 10^{-9} for 10.3125 and 12.5 Gbits/s operation are also indicated in the figure.

From Fig. 32, it can be seen that the maximum wireless distance to achieve a BER of 10^{-9} for 12.5 Gbits/s operation is approximately 1100 m for 99% link availability, 800 m for 99.99% link availability, and 500 m for 99.999% link availability.

9. Conclusions

We have described RoF research that is being carried out in the EU Network of Excellence ISIS (Infrastructures for broadband access in wireless/photonic and integration of strengths in Europe). This includes the investigation of both direct and external modulation and the use of single-mode and multimode fiber for the support of existing and emerging wireless networks.

Sections 2–4 detail a range of experimental work on the transmission of various wireless signal formats in RoF systems. Experiments have shown the feasibility of 1.25 Gbits/s IR-UWB transmission (using external modulation), with a BER of 10^{-9} being achieved for lengths of standard single-mode fiber up to 50 km. IR-UWB has also been transmitted over single-mode fiber by using an upconversion technique based on the nonlinear properties of low-cost 1550 nm wavelength VCSELs. In addition to the single-mode demonstrators, we have investigated transmission of multi-band UWB over multimode fiber. Despite signal degradation caused by intermodal dispersion, EVM measurements show that the ECMA-368 standard is satisfied for lengths up to 400 m.

As well as UWB transmission, experiments on the transmission of IEEE-standard wireless signals have been performed, namely, 802.11a (using upconversion with a view to its suitability for future millimeter-wave systems) and 802.11g (using low-cost multimode links that are suitable for in-building distribution systems). For the upconversion approach the dependence of EVM on both the VCSEL bias current and the RF/LO power ratio was investigated. It was found that for high LO powers the upconversion becomes less sensitive to bias current variations, and an optimal value of 7.4% EVM was found. For the multimode fiber approach, it was found that transmission over a 62.5 μm core fiber results in unacceptably high values of EVM, whereas use of a 50 μm core leads to an EVM of approximately 2.5% for fiber lengths up to 600 m, making it suitable for 802.11g transmission.

Multimode fiber links have also been evaluated for their suitability for RoF distribution of WiMAX signals. In this case, WiMAX measurements at the 3.5 GHz band over MMF remain below the standard limit for EVM up to 400 m, whereas UMTS measurements demonstrate conformance over the whole range and suggest an operational dynamic range of much greater than 35 dB. The UMTS ACLR requirements are 50 dB at 10 MHz offset and 45 dB at 5 MHz offset.

The simulation results in this paper concentrate on the performance of a basic RoF transmission system for 802.11a WLAN signals, under the presence of common optical noise contributors such as relative intensity noise (RIN), shot noise, fiber dispersion, and thermal noise. From the simulation of MZM modulation we were able to identify the optimal operating modulation index for the MZM. For the deployment of a local WLAN distribution system the results for transmit power requirement and receiver sensitivity show that a fiber span of 2–3 km would be able to deliver expected BER performance results for the system.

In addition to the physical layer experiments, the influence of higher layer protocols (such as MAC) on RoF performance has been examined. For example, if one considers the IEEE 802.11 MAC, the maximum fiber length will be limited by the ACK and clear-to-send time-out values. Both experiments and simulations have been conducted to look at the effect on throughput versus fiber length when using basic access, RTS/CTS, TCP, and UDP protocols.

We have demonstrated a wireless sensor network using RoF techniques. The feasibility of using radio over fiber to implement an 802.15.4 ZigBee network was exam-

ined. It was shown that a fiber length of up to 86 km is possible, but the time-out parameters of the MAC layer ACK signals must be taken into consideration. In particular, multiple MAC level checks are needed during network deployment in order to avoid time-out uncertainty due to clock jitter. Finally, we have developed a prototype broadband 60 GHz RoF demonstrator. This has been used to achieve transmission of up to 12.5 Gbits/s over distances of the order of 10 m in an indoor environment. The intended future application in this scenario would be home area networks, but outdoor experiments have also shown the ability for error-free (i.e., BER $<10^{-9}$) transmission up to 40 m. Calculations show that by using high-gain antennas (50 dBi), transmission up to approximately 1 km at a BER of 10^{-9} is possible for 12.5 Gbits/s operation with a 99% link availability.

Acknowledgments

The work reported has been partially funded by the European Union (EU) through the ISIS Network of Excellence (FP6-IST-026592). The authors acknowledge the many contributions of their collaborators in ISIS and particularly those of Anthony Nkansah, David Wake, Majlinda Mjeku, Roberto Llorente, Joaquin Pérez, Rubén Alemany, Jean-Pierre Vilcot, Bahman Kalantari-Sabet, and Mario Weiß.

References

1. M. Sauer, A. Kobayakov, and J. George, "Radio over fiber for picocellular network architectures," *J. Lightwave Technol.* **25**, 3301–3320 (2007).
2. D. Wake, M. Webster, G. Wimpenny, K. Beacham, and L. Crawford, "Radio over fiber for mobile communications," in *2004 IEEE International Topical Meeting on Microwave Photonics* (IEEE, 2004), pp. 157–160.
3. B. Cabon, "Recent Advances and Trends in European Projects on Microwave Photonics," in *The 5th Microwave and Millimeter-Wave Photonics Workshop* (IEICE, 2007).
4. ECMA-368 International Standard, "High rate ultra wideband PHY and MAC Standard," December 2007.
5. FCC 02-48, "Revision of part 15 of the Commission's rules regarding ultra-wideband transmission systems," April 2002.
6. A. L. Edwards, "The correlation coefficient," in *An Introduction to Linear Regression and Correlation* (W.H. Freeman, 1976), pp. 33–46.
7. M. Bennett, A. Flatman, and B. Tolley, "Broad market potential of 10 Gb/s Ethernet on FDDI grade MM fiber," IEEE802.3 (IEEE, 2004), available online at http://www.ieee802.org/3/tutorial/mar04/10GMMF_SG_v031604a.pdf.
8. Draka fibers data sheet, available online at http://www.draka.com/draka/Drakafiber/Languages/English/Navigation/Markets&Products/Technical_Support/Datasheets/DCOF_MaxCap-550.pdf.
9. Corning fibers data sheet, available online at http://www.corning.com/opticalfiber/products_applications/products/infincor.aspx.
10. Asahi Glass Perfluorinated GIPOF Lucina data sheet, available online at http://www.agc.co.jp/english/rd_e/e_lucina.html.
11. Chromis Perfluorinated GIPOF GigaPOF data sheet, available online at <http://www.chromisfiber.com/products.htm>.
12. C. Lethien, C. Loyez, and J.-P. Vilcot, "Potentials of radio over multimode fiber systems for the in-buildings coverage of mobile and wireless LAN applications," *IEEE Photon. Technol. Lett.* **17**, 2793–2795 (2005).
13. N. J. Gomes, A. Nkansah, and D. Wake, "Radio over MMF techniques, part I: RF to microwave frequency systems," Invited Paper, *J. Lightwave Technol.* **26**, 2388–2395 (2008).
14. D. Wake, A. Nkansah, C. Lethien, C. Sion, J.-P. Vilcot, and N. J. Gomes, "Optically-powered remote units for radio over fiber systems," *J. Lightwave Technol.* **26**, 2484–2491 (2008).
15. H. Al-Raweshidy and S. Komaki, *Radio over Fiber Technologies for Mobile Communications Networks* (Artech House, 2002).
16. B. J. Dixon, R. D. Pollard, and S. Iezekiel, "Orthogonal frequency-division multiplexing in wireless communication systems with multimode fiber feeds," *IEEE Trans. Microwave Theory Tech.* **49**, 1404–1409 (2001).
17. T. Kurt, A. Yongaçoğlu, and J.-Y. Chouinard, "OFDM and externally modulated multi-mode fibers in radio over fiber systems," *IEEE Trans. Wireless Commun.* **5**, 2669–2674 (2006).
18. D. K. Mynbaev and L. L. Scheiner, *Fiber-Optic Communications Technology* (Prentice-Hall, 2001).
19. IEEE Standard for Information Technology, Part 11 "802.11a, Wireless LAN Medium Access Control (MAC) and Physical Layer (PHY) Specifications: High-Speed Physical Layer Extension in the 5 GHz Band" (IEEE, 1999).
20. G. Singh and A. Alphones, "OFDM modulation study for a radio-over-fiber system for wireless LAN (802.11a)," in *Fourth International Conference on Information, Communications and Signal Processing/Fourth IEEE Pacific-Rim Conference on Multimedia* (IEEE, 2003), pp. 1460–1464.

21. M. Mjeku, B. Kalantari Sabet, J. E. Mitchell, and N. J. Gomes, "TCP and UDP performance over fibre-fed IEEE 802.11b networks," in *12th Microcoll Colloquium on Microwave Communications* (2007), pp. 89–92.
22. B. Kalantari Sabet, M. Mjeku, N. J. Gomes, and J. E. Mitchell, "Performance of TCP transmission over IEEE 802.11b network with long fibre distribution links," in *ISIS-IPHOBAC Workshop and Summer School*, Budapest, Hungary (2007).
23. B. Kalantari-Sabet and J. E. Mitchell, "MAC constraints on the distribution of 802.11 using optical fibre," in *Proceedings of the European Conference on Wireless Technology* (European Microwave Association, 2006), paper ECWT, poster-2 .
24. G. Bianchi, "Performance analysis of the IEEE 802.11 distributed coordination function," *IEEE J. Sel. Areas Commun.* **18**, 535–547 (2000).
25. M. Mjeku and N. J. Gomes, "Use of different acknowledgement policies for burst transmission in fiber-fed wireless LANs," *IEEE Commun. Lett.* **11**, 601–603 (2007).
26. R. Klinda, V. Bartoss, M. Csörnyei, T. Bánky, and T. Bercei, "General purpose combined optical-wireless ZigBee sensor networks," in *ICTON2007, 9th International Conference on Transparent Optical Networks* (IEEE, 2007), pp. 5–8.
27. N. J. Gomes, A. Das, A. Nkansah, M. Mjeku, and D. Wake, "Multimode fibre-fed indoor wireless networks," Invited Paper, in *IEEE International Topical Meeting in Microwave Photonics* (IEEE, 2006), pp. 1–4.
28. A. Stöhr, M. Weiß, V. Polo, R. Sambaraju, J. L. Corral, J. Marti, M. Huchard, B. Charbonnier, I. Siaud, S. Fedderwitz, and D. Jäger, "60 GHz radio-over-fiber techniques for 10 Gb/s broadband wireless transmission," in *Wireless World Research Forum*, Ottawa, Canada (WWRF, 2008).
29. M. Weiß, A. Stöhr, M. Huchard, S. Fedderwitz, B. Charbonnier, V. Rymanov, S. Babel, and D. Jäger, "60 GHz radio-over-fibre wireless system for bridging 10 Gb/s Ethernet links," in *European Conference and Exhibition on Optical Communication, ECOC 2008* (IEEE, 2008), pp. 143–144.